Accelerated Neuritogenesis and Maturation of Primary Spinal Motor Neurons in Response to Nanofibers

Caitlyn C. Gertz,[1]* Michelle K. Leach,[1,2,3] Lisa K. Birrell,[1] David C. Martin,[2,4]† Eva L. Feldman,[1] Joseph M. Corey[1,2,3]

[1] Department of Neurology, The University of Michigan, Ann Arbor, Michigan 48109

[2] Department of Biomedical Engineering, The University of Michigan, Ann Arbor, Michigan 48109

[3] Geriatrics Research, Education, and Clinical Center, VA Ann Arbor Healthcare Center, Ann Arbor, Michigan 48105

[4] Department of Materials Science and Engineering, The University of Michigan, Ann Arbor, Michigan 48109

Received 17 September 2009; revised 26 February 2010; accepted 4 March 2010

ABSTRACT: **Neuritogenesis, neuronal polarity formation, and maturation of axons and dendrites are strongly influenced by both biochemical and topographical extracellular components. The aim of this study was to elucidate the effects of polylactic acid electrospun fiber topography on primary motor neuron development, because regeneration of motor axons is extremely limited in the central nervous system and could potentially benefit from the implementation of a synthetic scaffold to encourage regrowth. In this analysis, we found that both aligned and randomly oriented submicron fibers significantly accelerated the processes of neuritogenesis and polarity formation of individual cultured motor neurons compared to flat polymer films and glass controls, likely due to restricted lamellipodia formation observed on fibers. In contrast, dendritic maturation and soma spreading were inhibited on fiber substrates after 2 days *in vitro*. This study is the first to examine the effects of electrospun fiber topography on motor neuron neuritogenesis and polarity formation. Aligned nanofibers were shown to affect the directionality and timing of motor neuron development, providing further evidence for the effective use of electrospun scaffolds in neural regeneration applications.** © 2010 Wiley Periodicals, Inc. Develop Neurobiol 70: 589–603, 2010

Keywords: **motor neuron; neuritogenesis; neuronal polarity; nanofibers; guidance; lamellipdodia**

INTRODUCTION

Striking variation in the size and morphology of neurons exists in the mammalian nervous system. Common to the all neurons is an architecture that allows the directional conduction of information. Multipolar neurons, which constitute the majority of neurons in the brain and include motor neurons and interneurons, possess a cell body with process extensions consisting of several dendrites and a single (usually longer) axon. Typically, electrical signals flow from dendrites to the cell body, and the resulting action potentials fired by the neuron are propagated down the axon to

Additional Supporting Information may be found in the online version of this article.

**Present address:* Neuroscience Graduate Program, University of California, San Francisco, CA 94143.

†*Present address:* Department of Materials Science and Engineering, University of Delaware, Newark, DE 19716.

Correspondence to: J.M. Corey (coreyj@umich.edu).

Contract grant sponsor: National Institute of Diabetes and Digestive and Kidney Diseases; contract grant number: DK020572.

Contract grant sponsor: NIH; contract grant number: K08 EB003996.

Contract grant sponsor: Army Research Office Multidisciplinary University Research Initiative (MURI) project; contract grant number: W911NF0610218.

Published online 8 March 2010 in Wiley InterScience (www.interscience.wiley.com).
DOI 10.1002/dneu.20792

exert effects on nearby synaptic targets, such as effector cells or other neurons (Craig and Banker, 1994).

Neuritogenesis, or the sprouting of neurites from a cell, is the first step in the development of a mature neuronal morphology (Dotti et al., 1988; Craig and Banker, 1994). This process, along with neurite growth and the development of dendrite-axon polarity, has been extensively studied through examination of the cytoskeleton (Sheetz et al., 1992; Isbister and O'Connor, 1999; Da Silva and Dotti, 2002), signaling mechanisms that drive neurite formation and growth (Da Silva and Dotti, 2002; Yoshimura et al., 2006; Arimura and Kaibuchi, 2007), competition among neurites for selection of the axon (Andersen and Bi, 2000; Arimura and Kaibuchi, 2005), and morphologies intermediate to the mature architecture of the neuron (Calderon de Anda et al., 2008). Importantly, *in vitro* studies have established the influence of soluble extracellular agents, such as WNT, netrin, and growth factors, on the speed of neurite growth, the number of neurites formed, and the generation of an axon or major neurite (Arimura and Kaibuchi, 2007). Biochemical components intrinsic to the extracellular substratum can affect neurite growth via integrin activation (Lochter et al., 1994; Lochter et al., 1995; Esch et al., 2000), as well as by affecting cell-to-substratum adhesiveness (Lochter et al., 1995).

In addition to the biochemical composition of the extracellular environment, the geometry of the extracellular matrix (ECM), arranged on the cell length scale, also affects neuritogenesis, neurite growth, and the establishment of dendrite-axon polarity. These architectural components include geometric patterns of multiple ECM components (Ma et al., 1998; Wheeler et al., 1999; Esch et al., 2000; Vogt et al., 2004; Shi et al., 2007), gradients of a single extracellular component in both two (Dertinger et al., 2002) and three dimensions (Dodla and Bellamkonda, 2006), and surface topography (Rajnicek et al., 1997; Dowell-Mesfin et al., 2004; Gomez et al., 2007a,b; Yao et al., 2009). Other factors affecting neurite growth include the influence of nearby target cells (Berman et al., 1993) and mechanical tension on existing neurites (Lamoureux et al., 2002; Pfister et al., 2004).

Electrospun fibers, a synthetic construct made from a variety of biocompatible and biodegradable polymers, can be fabricated to be nanometers in diameter to provide a unique extracellular geometry on the cell length scale. They have proven to be a powerful tool in guiding both developing and regenerating neurons *in vitro* and *in vivo* (Yang et al., 2005; Chew et al., 2007; Corey et al., 2007, 2008; Schnell et al., 2007; Kim et al., 2008). We have previously shown that topography presented by nanofibers profoundly affects neurite outgrowth of both primary motor and sensory neurons (Corey et al., 2007, 2008). Results from our earlier study revealed enhanced neurite outgrowth from dorsal root ganglia (DRG) explants when grown on aligned, unidirectional fibers compared to randomly oriented fibers. In addition, fiber alignment greatly affected DRG neurite orientation with increasing fiber alignment causing an increase in aligned, directed neurite outgrowth along the length of the fibers (Corey et al., 2007). Other studies published both before (Silva et al., 2004) and after (Christopherson et al., 2009; Xie et al., 2009) we began this study have demonstrated the effects of nanofiber topography on stem-cell differentiation and neurite outgrowth, revealing an enhanced capacity of stem cells to differentiate into neurons when cultured on nanofibers.

In this study, we aimed to elucidate the effects of polylactic acid (PLLA) electrospun fibers and their alignment on primary neuron neuritogenesis, neurite elongation, and the development of major and minor neurites. An electrospun scaffold recently designed by our group was used to produce both aligned and randomly oriented submicron fiber substrates (Corey et al., 2008). We chose to use primary motor neurons in our analysis instead of the more extensively studied hippocampal neurons because of their clear multipolar morphology as well as their relevance to clinical neurology and neural repair. Re-establishment of motor function is critical for the effective treatment of disability following neurological insult. However, regeneration of motor axons is extremely limited in the central nervous system (Stichel and Muller, 1998) and could potentially benefit from the implementation of a synthetic scaffold to encourage growth.

We found that aligned and randomly oriented fibers significantly accelerated spinal motor neuron neuritogenesis and major neurite (preaxon) growth compared to flat polymer films and glass controls, likely due to restricted lamellipodia formation that was observed on fibers. In contrast, the growth of minor neurites (predendrites), as well as soma spreading, was restricted on fiber substrates after 2 days *in vitro*. This study details the influence of tissue-engineered substrate topography on motor neuron neuritogenesis, neuronal polarity formation, and maturation of axons and dendrites. It also suggests principles by which extracellular topography can be manipulated using nanofiber scaffolds to help guide and rebuild both endogenous and transplanted neuronal connections during nervous system injury and disease.

MATERIALS AND METHODS

All materials were purchased from Sigma-Aldrich (St. Louis, MO) unless otherwise specified.

Electrospinning

PLLA with an inherent viscosity of 0.55–0.75 dL/g was obtained from Lactel Absorbable Polymers (Pelham, AL) and dissolved in chloroform to a concentration of ~4 wt %. In most cases, sulforhodamine 101 (Molecular Probes/Invitrogen, Carlsbad, CA) dissolved in chloroform to 1% (w/v) was added to the PLLA solution at a concentration of 0.5% [Fig. 1(A,C)] (Sun et al., 2007). The polymer solution was delivered by a KDS 100 syringe pump (KD Scientific, New Hope, PA) with a plastic needle and metal tip, to which an electrode is attached (spinnerette). A flow rate between 0.04 and 0.25 mL/h was used, with lower flow rates applied in more humid conditions to ensure collection of fibers with diameters below 1 μm. A voltage of 10 kV was applied by a high-voltage DC power supply (Hipotronics, Brewster, NY). The target wheel, constructed at the University of Michigan, is 10″ in diameter and has a beveled edge 0.0625″ wide. The wheel was grounded to attract the charged polymer. A motor (Caframo, Wiarton, ON) allowed varying the wheel rotation to affect fiber alignment. A 3–5-cm distance was maintained between the spinnerette and target wheel.

To collect aligned fibers, glass cover slips (22 × 22 mm sq., VWR, West Chester, PA) were taped to the wheel with double-sided masking tape, and a stripe of poly(lactic-*co*-glycolic acid) (PLGA, Lactel Absorbable Polymers, Pelham, AL) 85:15, dissolved to a concentration of 10% in chloroform, painted down the center immediately before electrospinning (Corey et al., 2008). The wheel was rotated at 285 rpm for 1–3 h to produce dense, aligned fiber bundles [Fig. 1(A,B)]. A stationary target consisting of a nail head embedded in a sheet of polycarbonate plastic with epoxy was used to collect randomly oriented fibers. A glass cover slip was taped down on the sides directly in front of the grounded nail head using double-sided masking tape. A square of PLGA 85:15 was painted onto cover slips, which were then subjected to electrospinning for ~15 min to produce a dense, random mesh of fibers [Fig. 1(C,D)]. The dramatic difference in fiber orientation between aligned and random fibers, as measured by fast Fourier transform and full width at half maximum, has been previously reported by our group (Corey et al., 2007), along with the hydrophobicity (contact angle) of PLLA fibers (Corey et al., 2008).

Scanning Electron Microscopy and Fiber Diameter Measurements

Polymer fibers were first coated with ~100 Å of gold/palladium by sputtering (Technics Hummer VI). Scanning electron microscopy (SEM) was conducted using an Amray

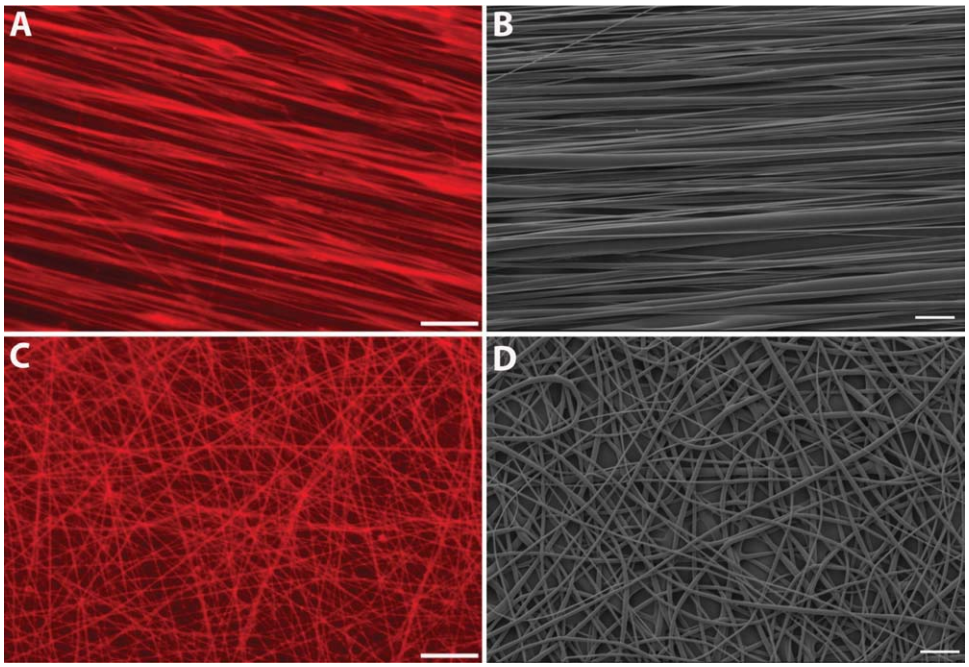

Figure 1 Aligned and randomly-oriented electrospun fiber substrates. Sulforhodamine-101 dye was incorporated into the polymer solution to aid in the visualization of neuronal interactions with fibers. Fluorescent images of aligned fibers [Fig. 1(A)] made by rotating the target wheel at 285 rpm and randomly oriented fibers [Fig. 1(C)] made using a stationary target. Representative SEM images [Fig. 1(B,D)] demonstrate the dramatic difference in fiber alignment produced by the two electrospinning techniques. Scale bar in A, C = 25 μm, scale bar in B, D = 10 μm.

1000-B, operating in high vacuum at 5 kV. Magnification images (2,000×) of both aligned and random fibers were acquired and fiber diameter measured using ImageJ [Fig. 1(B,D)]. Six samples of both aligned and random fibers were imaged and measurements performed on a minimum of five images per substrate. The mean ± standard deviation of aligned and random fiber diameters was 0.8047 μm ± 0.5746 and 0.6354 μm ± 0.4517, respectively.

Preparation of Cover Slips and PLLA Solvent-Cast Films

Glass cover slips were cleaned before use in cell culture. Cover slips were sonicated in 20% methanol solution for a minimum of 30 min. After three washes in deionized water, they were immersed in Piranha etch (7:3, concentrated sulfuric acid (70%): 30% hydrogen peroxide (30%)] overnight. After a 15-min wash in distilled water, cover slips were oven-dried at 55°C for at least 1 h.

To make polylactic acid (PLLA) solvent-cast films, a thin layer of PLGA 85:15, 10% in chloroform, was applied to glass cover slips and allowed to dry for at least 30 min. A layer of PLLA, 4% in chloroform, was then applied on top of the PLGA.

Substrate Coatings

All coatings were applied in a sterile, laminar flow hood. Substrates were coated with poly-L-lysine MW 150,000–300,000 at a concentration of 100 μg/mL for 1–3 h and then washed twice in sterile water.

Cell Culture

All experiments were done in accordance with the NIH Guide for Care and Use of Laboratory Animals as approved by the University Committee on Use and Care of Animals (UCUCA).

Primary motor neurons were cultured as has been previously described (Vincent et al., 2004; Corey et al., 2008). Briefly, perineural membranes were removed from spinal cords of E15 Sprague–Dawley rats and the tissue chopped into 2-mm pieces. Cells were dissociated by incubating in 0.05% trypsin/EDTA for 15 min at 37°C followed by gentle trituration for 1 min with a serum-coated, fire-polished glass Pasteur pipette. Motor neurons were isolated over 5.4% Optiprep in L-15 media by centrifugation for 15 min, 1000*g*. Motor neurons were collected from the top layer above the Optiprep. Cells were washed in L-15 media, then resuspended, and plated in culture medium. Neurobasal (Invitrogen) supplemented with 2% B27 (Invitrogen) was used as the culture medium with the following additives: 2.5 mg/mL albumin, 2.5 μg/mL catalase, 2.5 μg/mL superoxide dismutase, 0.01 mg/mL transferrin, 15 μg/mL galactose, 6.3 ng/mL progesterone, 16 μg/mL putrescine, 4 ng/mL selenium, 3 ng/mL β-estradiol, 4 ng/mL hydrocortisone, and 1× penicillin/streptomycin/neomycin. L-Glutamine (2 μM) was added to culture media immediately before plating. Cells were counted with trypan blue and the plating density determined from the number of live cells. Cells were plated at a density of 25 cells/mm^2, so that neurons would not contact one another. Using this protocol, our laboratory has identified greater than 90% of isolated cells as motor neurons by staining with antibodies against the motor neuron-specific markers islet-1 and SMI-32 (Vincent et al., 2004) as well as anticholine acetyltransferase (Corey et al., 2008).

Immunocytochemistry

Cells were fixed in 4% paraformaldehyde at RT for at least 15 min. To block nonspecific antibody binding, samples were incubated in 1% goat serum/1.25% BSA/0.05% Triton-X-100 in 1× PBS for 30 min. Primary antibodies, anti-neurofilament M 1:1000 (Millipore, Billerica, MA), TuJ1 1:500 (Neuromics, Edina, MN), MAP2 1:500 (Chemicon, Billerica, MA), and Tau 1:200 (Chemicon) were diluted in 10% goat serum/1% BSA/0.05% Triton-X-100/0.1% sodium azide in 1× PBS and incubated with cells overnight. The next day, the cells were washed in 1× PBS and incubated in appropriate secondary antibodies, Oregon Green 488 goat anti-rabbit (Invitrogen) 1:200 and rhodamine Red-X goat antimouse (Invitrogen) 1:200 diluted in 1× PBS, at RT for 2 h. For double-labeling with TuJ1 and Oregon Green 488 Phalloidin (Molecular Probes/Invitrogen), phalloidin was diluted 1:25 in 1× PBS and incubated with cells overnight at RT after secondary antibody staining. Prolong Gold (Molecular Probes/Invitrogen), an antifade agent with 4′,6-diamidino-2-phenylindole (DAPI), was used to stain nuclei.

Morphological Analysis and Stage Determination

Cells were fixed after 3, 6, 14, 24, 38, 48, and 96 h in culture and stained with antineurofilament M. Glass cover slips served as a control of which PLLA solvent-cast films, random fibers, and aligned fibers were compared. Images were taken on a Nikon Diaphot/FRET system and analyzed using the ImageJ freehand line tool. Only cells not contacting other cells and with DAPI staining revealing noncondensed nuclei were evaluated. For the aligned and random nanofibers, only cells in direct opposition to sulforhodamine 101-positive fibers were evaluated. The following morphological characteristics were scored: diameter of soma, presence of lamellipodia, and formation and length of neurites. Soma diameter was calculated by measuring the longest axis. The presence of lamellipodia was defined as a protrusion from the cell that did not qualify as a neurite. Neurite length was measured by tracing the trajectory of the neurite from the tip to the junction between the neurite and cell body. If a neurite exhibited branching, the measurement from the end of the longest branch to the soma was recorded. A neurite was defined as a process greater than or equal to the length of the soma diameter (Lochter et al., 1995). A major neurite was defined as a process greater than or equal to twice the

length of the soma diameter with the required presence of at least one other neurite. The remaining neurites of a cell possessing a major neurite were termed the minor neurites. Motor neurons were classified into five stages of development. A stage, 0–4, was assigned to each cell according to the following criteria (Dotti et al., 1988): stage 0 was defined as a completely rounded cell with no lamellipodia formation, stage 1 was defined as the presence of lamellipodia (and start of lamellipodia condensation) and no neurites, stage 2 was defined as the formation of a single neurite, stage 3 was defined as the presence of at least two neurites with no major neurite formation, and stage 4 was defined as the presence of at least two neurites with one qualifying as a major neurite (see Fig. 2). For the 3, 6, 14, and 24 h analysis, 128 ± 20 cells (mean ± standard deviation) from three independent experiments were analyzed per experimental condition (time and substrate type). For the 38, 48, and 96 h analysis, 106 ± 11 cells (mean ± standard deviation) from a minimum of two independent experiments were analyzed per experimental condition (time and substrate type).

Statistical Analysis

Statistics were performed using SAS® Software (Cary, NC). A mixed-model analysis of variance (ANOVA) with Bonferroni correction was performed on all measures with a numerical outcome. A logistic regression, and, in some cases, separate chi-square analyses with Fisher's exact two-sided probability test, was performed on measures with a yes/no outcome. Data were graphed using Prism software (GraphPad, La Jolla, CA) and are presented as mean ± SEM.

RESULTS

Neuritogenesis and Development of Motor Neurons on Glass

Our first objective was to establish the onset of neuritogenesis and neurite growth on planar glass substrates. This would allow comparing neuritogenesis and neurite growth on glass with that observed on fibers and verify that motor neurons have a similar developmental time-course as that observed for the *in vitro* development of hippocampal neurons (Dotti et al., 1988; Craig and Banker, 1994; Lochter et al., 1994; Lochter et al., 1995; Esch et al., 2000; Gomez et al., 2007a,b). We used a spinal cord motor neuron preparation, which results in over 90% of isolated cells identified as motor neurons (Vincent et al., 2004; Corey et al., 2008). Motor neurons were cultured on polylysine coated cover slips and examined first at 3 h after plating and then at various time intervals up to 96 h. Neurites were stained using neurofilament and nuclei using DAPI and cells assigned to a stage based on their morphology (see Materials and Methods section for the selection of cells to a specific stage).

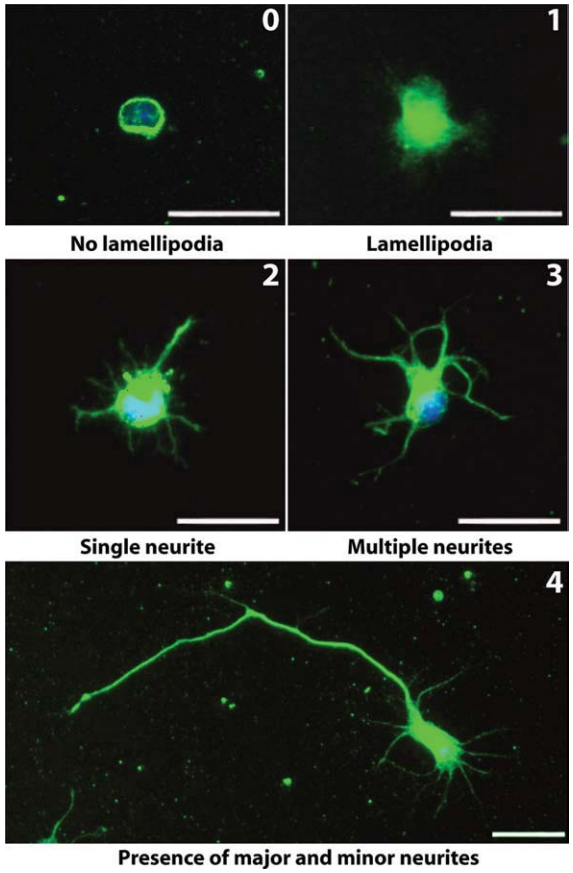

Figure 2 Characterization of motor neuron development. Five developmental stages (0–4) of motor neurons cultured on glass cover slips were defined based on the original classification of hippocampal neuron development by Dotti et al. (1988). Representative images of motor neurons in each stage are shown with the stage number written in the top, right-hand corner. Stage 0 was defined as a completely rounded cell with no lamellipodia formation, stage 1 was defined as the presence of lamellipodia (and start of lamellipodia condensation) and no neurites, stage 2 was defined as the formation of a single neurite, stage 3 was defined as the presence of at least two neurites with no major neurite formation, and stage 4 was defined as the presence of at least two neurites with one qualifying as a major neurite. Green, neurofilament; blue, DAPI; scale bar = 25 μm.

Figure 2 displays the typical sequence of events in cultured motor neuron development broken down into five stages, designated 0–4. Initially, cells land on the substrate devoid of any processes (stage 0). After a few hours, a lamellipodial membrane encircles the soma (stage 1). The lamellipodia condense into narrower processes that develop into neurites. Eventually, a single neurite develops (stage 2).

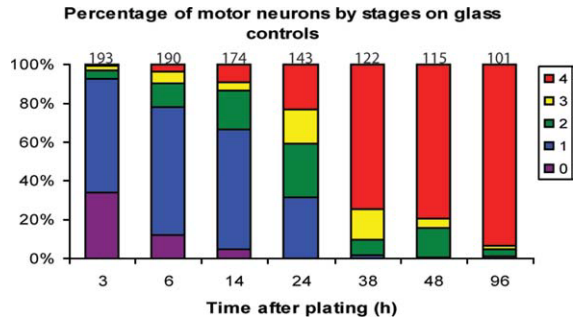

Figure 3 Time-course of motor neuron neuritogenesis and polarity formation on glass. The percentage of motor neurons on glass cover slips in each stage at different times in culture is illustrated in a 100% stacked column graph. The number of cells analyzed for each time-point is indicated above the stack. Red, stage 4; yellow, stage 3; green, stage 2; blue, stage 1; purple, stage 0.

After additional neurites develop (stage 3), a single neurite becomes predominant, growing faster than the others to become the major neurite (stage 4) and eventually the axon (Dotti et al., 1988).

The percentage of cells in each stage at various time points was calculated and plotted to elucidate the approximate time to reach each stage on glass controls [Fig. 3]. By 3 h, over 50% of motor neurons had lamellipodia, indicating that the majority of cells had reached stage 1 by 3 h. Stage 2 was not reached by a majority of neurons until 24 h, indicating that most neurons had extended at least one neurite between 14 and 24 h. Most of the neurons then developed multiple neurites (stage 3) as well as a major neurite (stage 4) by 38 h, indicating that these two processes occur in parallel for the majority of motor neurons analyzed. The percentage of motor neurons in stage 4 at 48 and 96 h was 79 and 93, respectively, indicating that neuronal polarity is further established at these later time points. The percentage of cells in each stage at these time points was also calculated and plotted for motor neurons grown on aligned and random nanofibers [Supporting Information Fig. 1(A,B), respectively].

Aligned and Random Fibers Accelerate Motor Neuron Neuritogenesis

We then compared the growth of motor neurons on random and aligned PLLA fibers to that on flat PLLA films and glass cover slips. Neurons grown on nanofibers developed neurites more quickly after plating. As seen in Figure 4, motor neurons grown on random and aligned PLLA fibers could be seen possessing several neurites by 14 h after plating, whereas motor neurons grown on glass and flat PLLA typically had no neurites at this time. In a direct comparison among

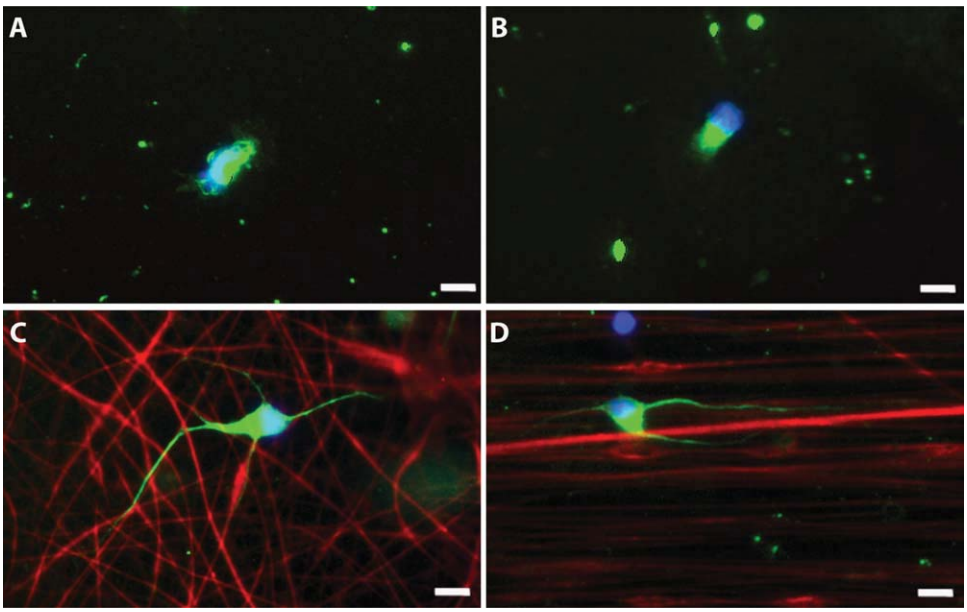

Figure 4 Representative images of motor neurons cultured for 14 h on control and fiber substrates. Motor neurons grown on glass (A), PLLA solvent-cast film (B), random fibers (C), and aligned fibers (D). At 14 h, less than 50% of cells have a neurite on both glass and PLLA solvent-cast films, with most cells in stage 1 exhibiting lamellipodia (A, B). In contrast, over 80% of cells possess a neurite on both random and aligned fibers at 14 h (C, D). Green, neurofilament; red(C, D), sulforhodamine 101-positive fibers; blue, DAPI; scale bar = 10 μm.

the four substrate types across four time points up to 24 h [Fig. 5(A)], a larger percentage of neurons on both aligned and random fibers (66% and 45%, respectively) had extended at least one neurite by 3 h compared to neurons on both flat substrates ($p < 0.0001$). This acceleration on fiber substrates continued between 6 and 14 h, but between 14 and 24 h more neurons grown on flat PLLA films and glass cover slips developed neurites, almost reaching the percentage of cells with neurites on nanofiber substrates by 24 h [Fig. 5(A)]. The logistic regression used to analyze these data revealed that both time ($p < 0.0001$) and substrate had a significant effect on neuritogenesis ($p < 0.0001$).

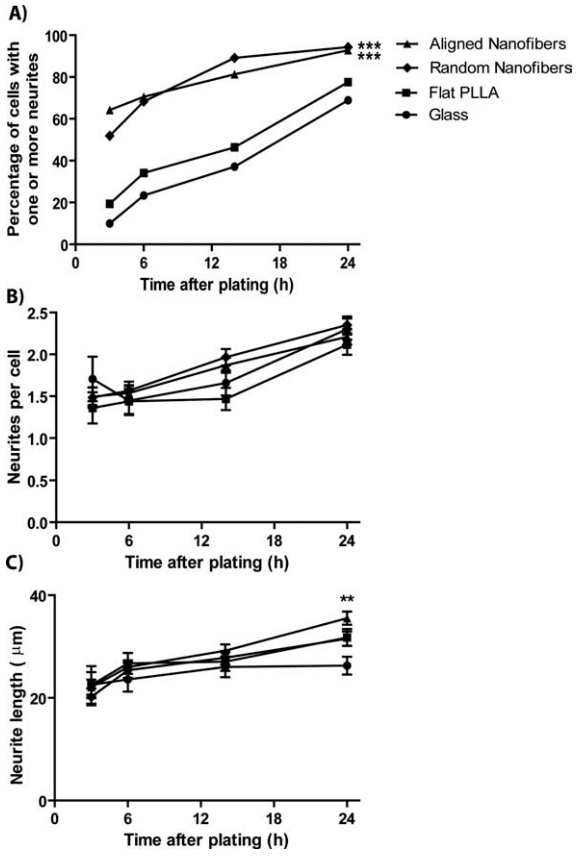

Figure 5 Motor neuron neuritogenesis is accelerated on aligned and random fibers. A: Up to 24 h, the percentage of cells with one or more neurites is significantly greater on random and aligned fibers when compared with glass and PLLA solvent-cast substrates. B: Of the cells possessing at least one neurite, the average number of neurites per cell is statistically equal for all substrates at these time points. C: Of the cells with at least one neurite, the average neurite length is statistically equal for all substrates at 3, 6, and 14 h. At 24 h, average neurite length on aligned fibers is statistically greater than the average neurite length on glass controls. $^{**}p < 0.01$, $^{***}p < 0.001$.

Next, we hypothesized that the neuritogenesis-promoting effect of the nanofibers would increase the number of neurites formed per cell. For cells possessing neurites, we compared the number of neurites per cell across the four substrates at four different time points. Using a mixed-model ANOVA test, we found that the average number of neurites per cell increased significantly over time ($p < 0.0001$), but that the average number of neurites formed per neuron did not differ among substrate types, contrary to our original hypothesis [Fig. 5(B)].

We wanted to see if nanofibers had an effect on the length of neurite outgrowth. Neurite length was equal among the four substrate types at 3, 6, and 14 h and differed only at 24 h [Fig. 5(C)]. At 24 h, average neurite length was longer on aligned fibers (35.5 μm) compared to glass controls (26.3 μm; $p = 0.002$), whereas neurite length on flat PLLA films (31.8 μm) and random fibers (31.5 μm) were statistically equal to that on aligned fibers.

Major Neurite Determination Is Accelerated on Nanofibers

After the formation of several minor neurites, the next stage we observed in motor neuron development was the formation of a major neurite, the precursor to an axon. We examined motor neurons on both nanofiber and planar substrates for the presence of a major neurite at four different time points. Within the first 24 h, nanofiber substrates revealed a greater percentage of cells possessing a major neurite compared to both planar PLLA and glass cover slips [$p < 0.0001$; Fig. 6(A)]. Although this finding is supported by logistic regression analysis for all the time points of observation, it was unclear whether there was a significant difference in major neurite formation between substrates at 3 h. To analyze this further, a Fisher's exact test of the 3 h data was performed revealing a greater percentage of cells with a major neurite on aligned fibers (14.2%) compared to both glass (0.7%, $p < 0.001$) and PLLA solvent-cast films (4%, $p = 0.003$). Similarly, significantly more cells on random fibers (9%) possessed a major neurite compared to glass ($p = 0.001$). There was no statistical difference in the percentage of cells with a major neurite between aligned and random fibers or between flat PLLA and glass at 3 h. The divergence in major neurite development between cells grown on fibers and planar surfaces is only temporary. By 38 h, between 75 and 85% of motor neurons on aligned fibers, random fibers, and glass controls exhibit neuronal polarity and were classified as stage 4 neurons.

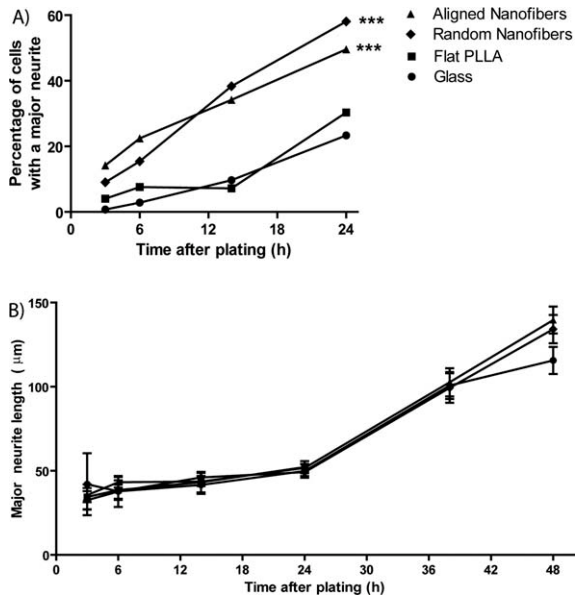

Figure 6 Major neurite formation occurs more rapidly on fibers. A: Between 3 and 24 h, the percentage of cells with a major neurite (defined as a process twice as long as the soma diameter and requiring the presence of at least one other neurite) is significantly greater on random and aligned fibers when compared to PLLA solvent-cast films and glass controls. B: Of the cells possessing a major neurite, the length of the major neurite is statistically equal on all substrates for all time points examined. ***$p < 0.001$.

This percentage increased to between 80 and 89% by 48 h (data not shown).

In line with our previous findings using DRG explants (Corey et al., 2007), we had hypothesized that nanofibers, specifically aligned nanofibers, would increase the length of the major neurite. A comparison of major neurite length among cells possessing a major neurite (stage 4) revealed that while major neurite length increased over time, substrate topography had no effect. Major neurite length was equal among all substrate types at each time point studied [Fig. 6(B)].

Dendritic Maturation and Soma Spreading Are Restricted on Nanofibers

On typical planar surfaces, such as glass, the number of minor processes extended by primary motor neurons increases with increasing time in culture. However, at later time points in our study, we found that the number of minor processes emanating from cells grown on fiber substrates appeared to be less than that of cells grown on planar surfaces. Among motor neurons with a clear difference between major and minor neurites (stage 4), there was a significant effect of topography on the number of minor neurites per cell at 38 and 48 h [$p < 0.0001$; Fig. 7(A)]. On average, motor neurons on glass controls had significantly more minor neurites per cell compared to neurons on both aligned and random fibers ($p < 0.0001$). The number of minor neurites was equal on both fiber orientations.

We also looked for a difference in minor neurite length at these same time points. There was a significant effect of time ($p < 0.0001$), topography ($p < 0.0001$), and a time-topography interaction ($p < 0.0001$) on average minor neurite length [Fig. 7(B)]. At 38 h, the average minor neurite length was equal on glass, aligned fibers, and random fibers. However, between 38 and 48 h, average minor neurite length on glass increased from 29.4 to 55.1 μm, whereas average minor neurite length on both aligned and random fibers did not differ appreciably [Fig. 7(B)]. Although the average minor neurite length nearly doubled on glass between 38 and 48 h, average major neurite length on glass remained at least twice as long as average minor neurite length at these time-points [Fig. 6(B)]. To confirm that the major and minor neurites are truly distinct and develop into mature axons and dendrites, respectively, we preformed immunocytochemistry using the axon-specific marker Tau and the dendrite-specific marker MAP2 on motor neurons grown on glass cover slips for 5DIV. As seen in Figure 7(C), MAP2 expression is restricted to the soma and minor neurites, whereas Tau expression is restricted to the major neurite indicating that minor and major neurites develop into mature dendrites and the axon, respectively.

Soma diameter was also decreased on fiber substrates. At 38 and 48 h, there was a significant effect of topography on soma diameter [$p < 0.0001$; Fig. 8(A)] that was not observed at earlier time points between 3 and 24 h (data not shown). Motor neurons on glass controls had significantly greater average soma diameters (15.7 μm) compared to those on aligned (14 μm, $p = 0.001$) and random fibers (13.6 μm, $p < 0.0001$). Soma diameter was statistically equal between the fiber substrates.

Representative images of stage 4 neurons at these later time points on glass, random fibers, and aligned fibers are illustrated in Figure 8(B,C,D), respectively. When comparing these images, one can see the restriction in soma spreading and dendritic maturation on fiber substrates. Similar to results found in our previous studies (Corey et al., 2007, 2008), more highly aligned fibers produced more highly aligned neurite outgrowth with neurites on aligned fibers clearly orientated along the length of the fibers

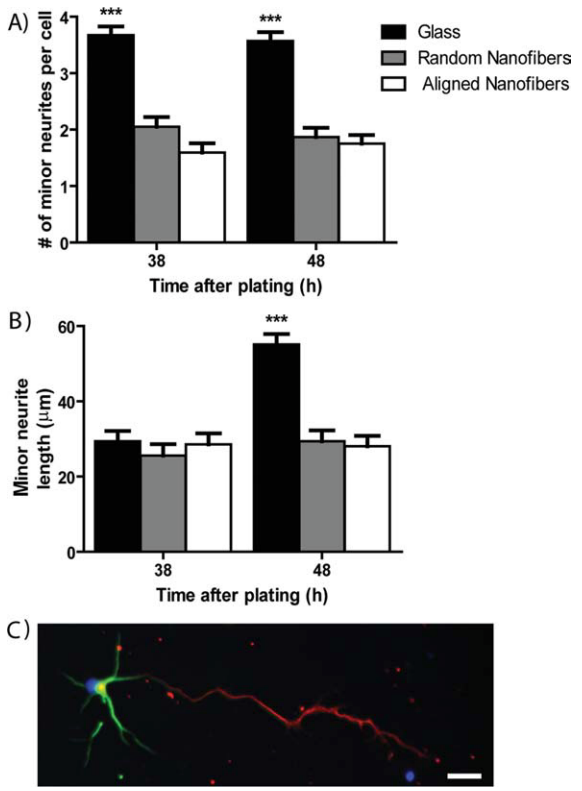

Figure 7 Dendrite formation and maturation is inhibited by fibers at 38 and 48 h in culture. Only stage 4 neurons have minor neurites, which include all neurites except the longest (major) neurite. A: The average number of minor neurites per cell is significantly greater on glass controls at 38 and 48 h compared to both aligned and random fibers. B: Average minor neurite length is statistically equal between glass and fiber substrates at 38 h but becomes significantly greater on glass controls compared to aligned and random fibers at 48 h. C: Representative image of a stage 4 motor neuron grown on glass for 5DIV and stained for the dendritic marker MAP2 (green) and axonal marker Tau (red). ***$p < 0.001$, scale bar = 25 μm.

[Fig. 8(D)]. Random fibers caused neurite outgrowth with inferior alignment [Fig. 8(C)] that more closely resembled neurite outgrowth on planar surfaces [Fig. 8(B)].

Lamellipodia Formation Differs on Nanofiber Substrates

The acceleration of neuritogenesis and major neurite development observed on the fiber substrates suggests that neuronal process extensions react differently on the nanofiber surface. When we analyzed neurons on all substrates within the first 24 h, no obvious lamellipodia were observed on the aligned nanofiber substrates. Therefore, we examined neurons after 1.5 h in culture to look for differences in lamellipodia formation of cells grown on the different substrate types (stage 1). On glass, the majority of motor neurons reveal flattened, veil-like lamellipodia structures that often surround the entire cell cytoplasm (see Fig. 9) (Dotti et al., 1988; Caceres et al., 1992). In contrast, cells on fibers extended filipodia-like structures that rarely surrounded the entire cell perimeter. Instead, these early processes budded from specific regions of the cell, typically along fibers just adjacent to the cell body (Fig. 9, arrows). Fewer lamellipodia extended from cells on fibers and instead of a widened, flattened morphology, they appeared narrower, resembling immature neurites.

DISCUSSION

Nanofibers direct regenerating neurites *in vitro* (Yang et al., 2005; Corey et al., 2007, 2008; Kim et al., 2008) and *in vivo* in peripheral nerve (Chew et al., 2007; Kim et al., 2008). They may be useful for many applications involving neuronal guidance in injured nervous tissue, including in the spinal cord and brain. We hypothesized that neurons in contact with nanofibers would develop neurites sooner than neurons grown in similar microenvironments lacking such cell-length scale cues. The critical finding in this study is that nano- and submicron fibers accelerate the development and maturation of spinal cord motor neurons. Development of initial neurites was more rapid on fibers compared to glass or planar PLLA films, but there was no difference in the number or length of neurites that developed. Considering results from our earlier work regarding neurite outgrowth from DRG explants on nanofibers (Corey et al., 2007), we were surprised to find that neurites from motor neurons were equal in length and number on both aligned and random nanofiber orientations. Additionally, major neurites developed sooner on fibers indicating an overall acceleration of neuronal maturation when these topographical cues are present, similar to that shown with Schwann cells (Chew et al., 2008). However, minor neurite elaboration after 2 days of growth was reduced on the nanofiber substrates both in terms of number and length. To our knowledge, this is the first study assessing the development of primary motor neurons on electrospun fibers in serum-free culture conditions. These results confirm the results of others that have demonstrated a strong topographical influence on neuronal development (Yang et al., 2005; Gomez et al., 2007a,b) and show that nanofibers cannot only profoundly influence the directionality of neurite outgrowth but also

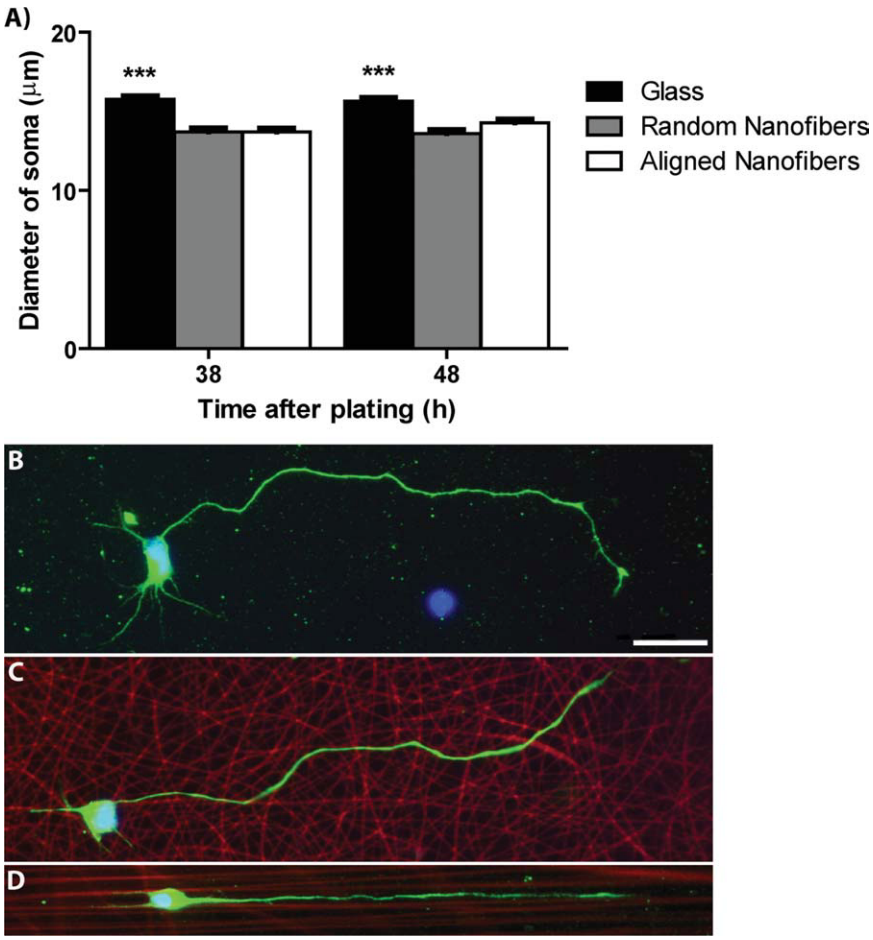

Figure 8 Soma spreading is restricted on aligned and random fibers at 38 and 48 h in culture. A: Soma diameter is significantly greater on glass controls compared to aligned and random fibers at 38 and 48 h. B: Representative image of a stage 4 motor neuron cultured for ~2 days on glass. At least three minor neurites are visible in addition to a longer, major neurite. C: Representative image of a stage 4 motor neuron cultured for ~2 days on randomly-oriented fibers. Only two minor neurites are visible in addition to a major neurite. D: Representative image of a stage 4 motor neuron cultured for ~2 days on aligned fibers. Only two minor neurites and a major neurite are visible, all growing parallel to the fibers. A: ***$p < 0.001$. B, C, D: Green, neurofilament; red, sulforhodamine 101-positive fibers; blue, DAPI; scale bar = 25 μm.

accelerate the processes of neuritogenesis and major neurite determination.

The development of primary neurons in low-density culture was first investigated by Dotti and Banker using hippocampal neurons (Dotti et al., 1988). Subsequent studies of development and synaptic plasticity have typically been performed in hippocampal neuron cultures (Rao et al., 2000; Banker, 2003; Graf et al., 2004; Das and Banker, 2006; Linhoff et al., 2009). We found no detailed, published depiction of cultured motor neuron development in the literature. Therefore, we began our study by characterizing motor neuron growth on glass to see how similar their *in vitro* development was to that of hippocampal neurons. Data from these observations would also serve as a baseline for comparing motor neuron growth on glass to that on nanofiber substrates. Damage to motor neurons caused by stroke, trauma (e.g., spinal cord and peripheral nerve injury), and motor neuron disease (e.g., amyotrophic lateral sclerosis) results in weakness and lack of mobility. Because replacing lost motor neuron connections is critical for reestablishing motor abilities following injury, we chose to use motor neurons in this study.

Motor neurons follow a very similar developmental sequence as hippocampal neurons *in vitro* including cell attachment, formation of lamellipodia, condensation of lamellipodia into neurites, growth of the

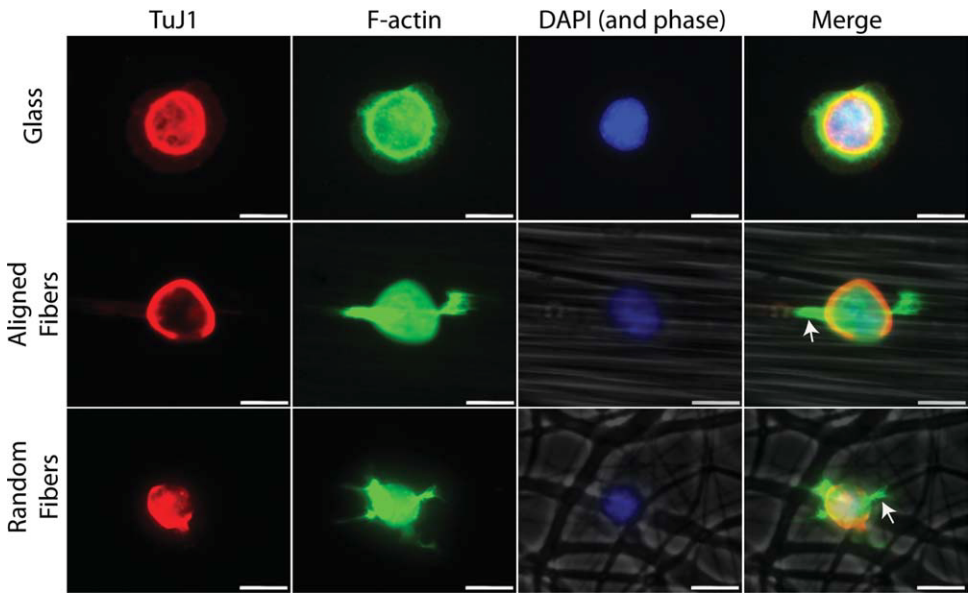

Figure 9 Lamellipodia formation is spatially restricted on fibers. Motor neurons were grown on glass, aligned fibers, and random fibers and fixed after 1.5 h in culture. Cells were stained with phalloidin (green), TuJ1 (red), and DAPI (blue) to visual lamellipodia. Aligned and random fibers were imaged in phase-contrast and included in the merged image. Flattened, veil-like lamellipodia were observed on glass while lamellipodia typically formed only along fibers just adjacent to the cell body (arrows). Scale bar = 10 μm.

first neurite followed by extension of additional neurites, and the selection of a major neurite that eventually becomes the axon (see Fig. 2). However, the time course of these events differed between the two cell types. In our system, motor neurons formed lamellipodia faster (by 3 h as opposed to 6 h), but they formed multiple neurites more slowly (by 38 h as opposed to 12 h). This could be due to intrinsic differences in spinal motor and hippocampal neurons, the latter cell type being known for greater and more elaborate dendritic growth than motor neurons. Alternatively, the initial use of serum and a glial feeder layer in the hippocampal culture system that is absent from our system may provide ECM and growth factors that speed neurite outgrowth. However, these differences apparently have no effect on major neurite (axon) development, because the timing of major neurite development did not differ between cell types (Dotti et al., 1988). Additional factors contributing to the slower neurite development of motor neurons could be our low-cell plating density (25 cells/mm^2) that increased the distance between neurons, lowering local concentrations of trophic factors (Brewer et al., 1993).

The development and growth of neurites follow a sequence of complex intrinsic cell-signaling events (Da Silva and Dotti, 2002; Arimura and Kaibuchi, 2007). However, the signaling mechanisms that govern neuritogenesis can be influenced by neuronal interactions with the biochemistry (Lochter et al., 1994; Lochter et al., 1995; Gomez et al., 2007a,b), geometry (Corey et al., 1991; Britland et al., 1992; Wheeler et al., 1999; Shi et al., 2007), and topography (Rajnicek et al., 1997; Yang et al., 2005; Gomez et al., 2007a,b) of the extracellular environment. In this study, we found that the topographical influence of both aligned and random fibers accelerates neuritogenesis [Fig. 5(A)]. When considering the highly concentrated polylysine solution with which all surfaces were coated (Wheeler and Brewer, 1994; Lochter et al., 1995), as well as the low-cell plating density used to minimize the effects of trophic factors seen at higher densities (Brewer et al., 1993), this effect is particularly dramatic. Our results corroborate those seen by Gomez et al. (2007a,b) who observed an enhancement in hippocampal neuron axonogenesis as a result of micron-sized channels.

In contrast to our previous finding of longer neurite outgrowth from DRG explants on aligned fibers compared to random nanofibers (Corey et al., 2007), we found neurite length of motor neurons to be equal on both fiber orientations [Fig. 5(C)]. These results are also in contrast with Yang et al. (2005), who observed an increase in C17.2 neurite length on

aligned nanofibers compared to random nanofibers, although these results were obtained using fibers with significantly smaller diameters. Although we hypothesized that random fibers would increase the number of neurites formed per cell, average neurite number was the same on random and aligned fibers [Fig. 5(B)]. Similarly, this may be due to the relative diameter of the nanofibers. Nanofibers with smaller diameters may provide more pathways on which lamellipodia could condense along and form neurites. From our results, it appears that compared to flat PLLA films or glass controls our fiber substrates decrease the latency between neuronal attachment and neuritogenesis but do not affect the number or length of neurites.

Biochemistry, geometry, and topography not only affect neuritogenesis, but also the development of the major neurite that eventually matures into the axon (Lochter et al., 1995; Esch et al., 1999, 2000; Dertinger et al., 2002; Gomez et al., 2007a,b). Similar to the initial process of neuritogenesis, we found that electrospun fibers profoundly accelerated the development of major neurites, with motor neurons grown on fibers developing a major neurite 2.5–3 times as fast as those grown on glass [Fig. 6(A)]. However, as seen with initial neurite formation, fibers did not speed major neurite growth, because average major neurite length was equal on all surfaces. It is possible that with longer durations of growth in culture that a difference in major neurite length may be observed, because we measured neurites only through 48 h in this study. Nonetheless, our results are consistent with those of Gomez et al. (2007b) who observed a dissociation between enhancement of neuronal polarity and neurite length on microfabricated topographical surfaces. Hippocampal neurons grown on microchannels 1 and 2-μm wide exhibited accelerated axonogenesis, whereas axon length was only increased when the biochemical signal NGF was immobilized to the microchannels.

Cells exhibit different properties in three compared to two dimensions (Cukierman et al., 2001). We hypothesize that the smaller soma size observed on nanofibers, as measured by the longest axis of the motor neuron cell body, is due to the three-dimensional shape of the substrate created by the fibers [Fig. 8(A)]. Cells likely reside in the spaces, or valleys, between fibers as it has also been shown that neurites grow in these regions (Nisbet et al., 2007). Neurons migrate until the cell body localizes on an adhesive region that approximates the area of a cell (Corey et al., 1991). Therefore, it is likely that cell bodies preferentially adhere to valleys between fibers that tend to have a larger surface area. Our measurements reflect an effective decrease in cell spreading, because part of the cytoplasm is likely located in the spaces between fibers, which are restricted in size.

Dendrite maturation occurs after minor processes develop during neuritogenesis and axonal polarity is initiated (Dotti et al., 1988). Even though our analysis only extended to 48 h, we found that dendrite development on fibers was decreased at this later time period. Between 3 and 24 h, the number of neurites per cell on glass and fibers was equal, averaging between 1.5 and 2.3 [Fig. 5(B)]. However, between 24 and 38 h, the average number of minor neurites on glass increased to four per cell, whereas neurons on fibers continued to possess only two minor neurites per cell on average [Fig. 7(A)]. Length of minor neurites was similarly affected, averaging $\sim$30 μm on fibers between 38 and 48 h, whereas this length doubled for cells grown on glass over this time interval [Fig. 7(B)]. These data suggest that neurons on fibers are restricted from developing multiple neurites between 24 and 48 h and that elongation of minor neurites on fibers is limited during this time interval. One possible explanation for this finding is that surfaces with nanotopographical features keep cells in an axon growth program, delaying or limiting dendrite development altogether. Such a finding could prove advantageous for regeneration in the central nervous system, where neurons exhibit slower axon growth once dendrites have developed (Condic, 2002). Another possibility is that it is more difficult for cell bodies located among fibers to extend neurites. Alternatively, our observed differences may be accounted for by our low-cell density or by the timing of observation. Evidence for this comes from our qualitative observation that motor neurons grown on aligned nanofibers appear to have greater dendrite outgrowth when cultured for 4 days at twice the plating density used in this study (Corey et al., 2008), but this has not yet been confirmed quantitatively.

The events that allow a neuron to break its initial spherical shape to form neurites are not completely understood. However, it is widely believed that the basic engine for the process of lamellipodia and neurite formation is the actin cytoskeleton (Sheetz et al., 1992; Isbister and O'Connor, 1999; Da Silva and Dotti, 2002). Communication between the membrane and actin is implicated in the initial stages of neuritogenesis (Da Silva and Dotti, 2002). We rarely observed a full, circular ribbon of lamellipodia around neurons on aligned fibers even after only 3 h in culture. Therefore, we stained neurons to visualize both tubulin and the actin cytoskeleton to examine this process at even earlier time points. After only 1.5 h in culture, actin is localized to very small regions just adjacent to the cell body along aligned and random fibers instead

of being extended circumferentially as seen on flat surfaces (see Fig. 9). On both aligned and random fibers, processes resembling filopodia seem to be extending along fibers. The localization of actin to specific regions as early as 1.5 h after plating demonstrates a dramatic effect of fiber topography on the initial stages of neuritogenesis and may account for the accelerated neuritogenesis observed on these substrates. Experiments are currently underway to visualize this process in real time to examine which components of the cytoskeleton are expressed in these process extensions at this early developmental stage.

This study is the first detailed account of neuritogenesis, neuronal polarity formation, and axonal and dendritic maturation of motor neurons on electrospun nanofiber scaffolds. We have demonstrated the ability of PLLA nanofibers of varying alignment to accelerate neuritogenesis and neuronal polarity formation of motor neurons. These findings, along with our previous observations demonstrating the profound effects of fiber alignment on the directionality of neurite outgrowth (Corey et al., 2007, 2008), provide further support for the use of nanofiber scaffolds to aid in the regeneration and guidance of both endogenous and transplanted neurons following neurological insult. However, the ability of fiber topography to provide guidance and directional cues to cells must be weighted against possible implications of dendritic and soma restriction. Future studies will look at the effects of fiber topography, including fiber density, and diameter, in conjunction with the biochemical composition of the fibers, such as the incorporation of ECM proteins and growth factors (Chew et al., 2007; Koh et al., 2008), on neuronal development, growth, and guidance with the hope of developing an effective and reliable nanofiber scaffold for neural regeneration applications.

This work used the Morphology and Image Analysis Core of the Michigan Diabetes Research and Training Center and the authors would like to thanks Dr. Stephen I. Lentz, the Core's Laboratory Director, for his valuable assistance. The authors also thank Kenneth Guire at the University of Michigan Center for Statistical Consultation and Research for assistance with the statistical analysis, Dr. Lorene Lanier of the University of Minnesota for assistance with immunocytochemistry, Dr. Jeffrey Hendricks for helpful discussions, and Denice Janus for assistance with electronic submission.

REFERENCES

Andersen SS, Bi GQ. 2000. Axon formation: A molecular model for the generation of neuronal polarity. Bioessays 22:172–179.

Arimura N, Kaibuchi K. 2005. Key regulators in neuronal polarity. Neuron 48:881–884.

Arimura N, Kaibuchi K. 2007. Neuronal polarity: From extracellular signals to intracellular mechanisms. Nat Rev Neurosci 8:194–205.

Banker G. 2003. Pars, PI 3-kinase, and the establishment of neuronal polarity. Cell 112:4–5.

Berman SA, Moss D, Bursztajn S. 1993. Axonal branching and growth cone structure depend on target cells. Dev Biol 159:153–162.

Brewer GJ, Torricelli JR, Evege EK, Price PJ. 1993. Optimized survival of hippocampal neurons in B27-supplemented Neurobasal, a new serum-free medium combination. J Neurosci Res 35:567–576.

Britland S, Clark P, Connolly P, Moores G. 1992. Micropatterned substratum adhesiveness: A model for morphogenetic cues controlling cell behavior. Exp Cell Res 198: 124–129.

Caceres A, Mautino J, Kosik KS. 1992. Suppression of MAP2 in cultured cerebellar macroneurons inhibits minor neurite formation. Neuron 9:607–618.

Calderon de Anda F, Gartner A, Tsai LH, Dotti CG. 2008. Pyramidal neuron polarity axis is defined at the bipolar stage. J Cell Sci 121:178–185.

Chew SY, Mi R, Hoke A, Leong KW. 2007. Aligned protein-polymer composite fibers enhance nerve regeneration: A potential tissue-engineering platform. Adv Funct Mater 17:1288–1296.

Chew SY, Mi R, Hoke A, Leong KW. 2008. The effect of the alignment of electrospun fibrous scaffolds on Schwann cell maturation. Biomaterials 29:653–661.

Christopherson GT, Song H, Mao H-Q. 2009. The influence of fiber diameter of electrospun substrates on neural stem cell differentiation and proliferation. Biomaterials 30:556–564.

Condic ML. 2002. Neural development: Axon regeneration derailed by dendrites. Curr Biol 12:R455–R457.

Corey JM, Gertz CC, Wang BS, Birrell LK, Johnson SL, Martin DC, Feldman EL. 2008. The design of electrospun PLLA nanofiber scaffolds compatible with serum-free growth of primary motor and sensory neurons. Acta Biomater 4:863–875.

Corey JM, Lin DY, Mycek KB, Chen Q, Samuel S, Feldman EL, Martin DC. 2007. Aligned electrospun nanofibers specify the direction of dorsal root ganglia neurite growth. J Biomed Mater Res A 83:636–645.

Corey JM, Wheeler BC, Brewer GJ. 1991. Compliance of hippocampal neurons to patterned substrate networks. J Neurosci Res 30:300–307.

Craig AM, Banker G. 1994. Neuronal polarity. Annu Rev Neurosci 17:267–310.

Cukierman E, Pankov R, Stevens DR, Yamada KM. 2001. Taking cell-matrix adhesions to the third dimension. Science 294:1708–1712.

Da Silva JS, Dotti CG. 2002. Breaking the neuronal sphere: Regulation of the actin cytoskeleton in neuritogenesis. Nat Rev Neurosci 3:694–704.

Das SS, Banker GA. 2006. The role of protein interaction motifs in regulating the polarity and clustering of the

metabotropic glutamate receptor mGluR1a. J Neurosci 26:8115–8125.

Dertinger SK, Jiang X, Li Z, Murthy VN, Whitesides GM. 2002. Gradients of substrate-bound laminin orient axonal specification of neurons. Proc Natl Acad Sci USA 99:12542–12547.

Dodla MC, Bellamkonda RV. 2006. Anisotropic scaffolds facilitate enhanced neurite extension in vitro. J Biomed Mater Res A 78:213–221.

Dotti CG, Sullivan CA, Banker GA. 1988. The establishment of polarity by hippocampal neurons in culture. J Neurosci 8:1454–1468.

Dowell-Mesfin NM, Abdul-Karim MA, Turner AM, Schanz S, Craighead HG, Roysam B, Turner JN, Shain W. 2004. Topographically modified surfaces affect orientation and growth of hippocampal neurons. J Neural Eng 1:78–90.

Esch T, Lemmon V, Banker G. 1999. Local presentation of substrate molecules directs axon specification by cultured hippocampal neurons. J Neurosci 19:6417–6426.

Esch T, Lemmon V, Banker G. 2000. Differential effects of NgCAM and N-cadherin on the development of axons and dendrites by cultured hippocampal neurons. J Neurocytol 29:215–223.

Gomez N, Chen S, Schmidt CE. 2007a. Polarization of hippocampal neurons with competitive surface stimuli: Contact guidance cues are preferred over chemical ligands. J R Soc Interf 4:223–233.

Gomez N, Lu Y, Chen S, Schmidt CE. 2007b. Immobilized nerve growth factor and microtopography have distinct effects on polarization versus axon elongation in hippocampal cells in culture. Biomaterials 28:271–284.

Graf ER, Zhang X, Jin SX, Linhoff MW, Craig AM. 2004. Neurexins induce differentiation of GABA and glutamate postsynaptic specializations via neuroligins. Cell 119:1013–1026.

Isbister CM, O'Connor TP. 1999. Filopodial adhesion does not predict growth cone steering events in vivo. J Neurosci 19:2589–2600.

Kim YT, Haftel VK, Kumar S, Bellamkonda RV. 2008. The role of aligned polymer fiber-based constructs in the bridging of long peripheral nerve gaps. Biomaterials 29:3117–3127.

Koh HS, Yong T, Chan CK, Ramakrishna S. 2008. Enhancement of neurite outgrowth using nano-structured scaffolds coupled with laminin. Biomaterials 29:3574–3582.

Lamoureux P, Ruthel G, Buxbaum RE, Heidemann SR. 2002. Mechanical tension can specify axonal fate in hippocampal neurons. J Cell Biol 159:499–508.

Linhoff MW, Lauren J, Cassidy RM, Dobie FA, Takahashi H, Nygaard HB, Airaksinen MS, Strittmatter SM, Craig AM. 2009. An unbiased expression screen for synaptogenic proteins identifies the LRRTM protein family as synaptic organizers. Neuron 61:734–749.

Lochter A, Taylor J, Braunewell KH, Holm J, Schachner M. 1995. Control of neuronal morphology in vitro: Interplay between adhesive substrate forces and molecular instruction. J Neurosci Res 42:145–158.

Lochter A, Taylor J, Fuss B, Schachner M. 1994. The extracellular matrix molecule janusin regulates neuronal morphology in a substrate- and culture time-dependent manner. Eur J Neurosci 6:597–606.

Ma W, Liu QY, Jung D, Manos P, Pancrazio JJ, Schaffner AE, Barker JL, Stenger DA. 1998. Central neuronal synapse formation on micropatterned surfaces. Brain Res Dev Brain Res 111:231–243.

Nisbet DR, Pattanawong S, Ritchie NE, Shen W, Finkelstein DI, Horne MK, Forsythe JS. 2007. Interaction of embryonic cortical neurons on nanofibrous scaffolds for neural tissue engineering. J Neural Eng 4:35–41.

Pfister BJ, Iwata A, Meaney DF, Smith DH. 2004. Extreme stretch growth of integrated axons. J Neurosci 24:7978–7983.

Rajnicek A, Britland S, McCaig C. 1997. Contact guidance of CNS neurites on grooved quartz: Influence of groove dimensions, neuronal age and cell type. J Cell Sci 110 (Pt 23):2905–2913.

Rao A, Cha EM, Craig AM. 2000. Mismatched appositions of presynaptic and postsynaptic components in isolated hippocampal neurons. J Neurosci 20:8344–8353.

Schnell E, Klinkhammer K, Balzer S, Brook G, Klee D, Dalton P, Mey J. 2007. Guidance of glial cell migration and axonal growth on electrospun nanofibers of poly-ε-caprolactone and a collagen/poly-ε-caprolactone blend. Biomaterials 28:3012–3025.

Sheetz MP, Wayne DB, Pearlman AL. 1992. Extension of filopodia by motor-dependent actin assembly. Cell Motil Cytoskeleton 22:160–169.

Shi P, Shen K, Kam LC. 2007. Local presentation of L1 and N-cadherin in multicomponent, microscale patterns differentially direct neuron function in vitro. Dev Neurobiol 67:1765–1776.

Silva GA, Czeisler C, Niece KL, Beniash E, Harrington DA, Kessler JA, Stupp SI. 2004. Selective differentiation of neural progenitor cells by high-epitope density nanofibers. Science 303:1352–1355.

Stichel CC, Muller HW. 1998. Experimental strategies to promote axonal regeneration after traumatic central nervous system injury. Prog Neurobiol 56:119–148.

Sun T, Norton D, McKean RJ, Haycock JW, Ryan AJ, MacNeil S. 2007. Development of a 3D cell culture system for investigating cell interactions with electrospun fibers. Biotechnol Bioeng 97:1318–1328.

Vincent AM, Mobley BC, Hiller A, Feldman EL. 2004. IGF-I prevents glutamate-induced motor neuron programmed cell death. Neurobiol Dis 16:407–416.

Vogt AK, Stefani FD, Best A, Nelles G, Yasuda A, Knoll W, Offenhausser A. 2004. Impact of micropatterned surfaces on neuronal polarity. J Neurosci Methods 134:191–198.

Wheeler BC, Brewer GJ. 1994.Selective hippocampal neuritogenesis: Axon growth on laminin or pleiotrophin, dendrite growth on poly-D-lysine. In Proceedings of Society for Neuroscience Abstracts, Miami Beach, FL, p 1292.

Wheeler BC, Corey JM, Brewer GJ, Branch DW. 1999. Microcontact printing for precise control of nerve cell growth in culture. J Biomech Eng 121:73–78.

Xie J, Willerth SM, Li X, Macewan MR, Rader A, Sakiyama-Elbert SE, Xia Y. 2009. The differentiation of embryonic stem cells seeded on electrospun nanofibers into neural lineages. Biomaterials 30:354–362.

Yang F, Murugan R, Wang S, Ramakrishna S. 2005. Electrospinning of nano/micro scale poly(L-lactic acid) aligned fibers and their potential in neural tissue engineering. Biomaterials 26:2603–2610.

Yao L, Wang S, Cui W, Sherlock R, O'Connell C, Damodaran G, Gorman A, Windebank A, Pandit A. 2009. Effect of functionalized micropatterned PLGA on guided neurite growth. Acta Biomater 5:580–588.

Yoshimura T, Arimura N, Kaibuchi K. 2006. Signaling networks in neuronal polarization. J Neurosci 26:10626–10630.